Chirality Remote Control in Nanoporous Materials by Circularly Polarized Light

Kanj, A. B.; Bürck, J.; Vankova, N.; Li, C.; Mutruc, D.; Chandresh, A.; Hecht, S.; Heine, T.; Heinke, L.;

Originally published:

April 2021

Journal of the American Chemical Society 143(2021)18, 7059-7068

DOI: https://doi.org/10.1021/jacs.1c01693

Chirality Remote Control in Nanoporous Materials by Circularly Polarized Light

Anemar Bruno Kanj, Jochen Bürck, Nina Vankova, Chun Li, Dragos Mutruc, Abhinav Chandresh, Stefan Hecht, Thomas Heine, and Lars Heinke*

ABSTRACT: The ability to dynamically control chirality remains a grand challenge in chemistry. Although many molecules possess chiral isomers, lacking their isolation, for instance during photoisomerization, results in racemic mixtures with suppressed enantiospecific chiral properties. Here, we present a nanoporous solid in which chirality and enantioselective enrichment is induced by circularly polarized light (CPL). The material is based on photoswitchable fluorinated azobenzenes attached to the scaffold of a crystalline metal−organic framework (MOF). The azobenzene undergoes *trans* to *cis* photoisomerization upon irradiation with green light and reverts back to *trans* upon violet light. While each moiety in *cis* conformation is chiral, we show the *trans* isomer also possesses a nonplanar, chiral conformation. During photoisomerization with unpolarized light, no enantiomeric enrichment is observed and both isomers, *R* and *S cis* as well as *R* and *S trans*, respectively, are formed in identical quantities. In contrast, CPL causes chiral photoresolution, resulting in an optically active material. Right CPL selectively excites *R cis* and *R trans* enantiomers, producing a MOF with enriched *S* enantiomers, and *vice versa*. The induction of optical activity is reversible and only depends on the light handedness. As shown by first principle DFT calculations, while both, *trans* and *cis*, are stabilized in nonplanar, chiral conformations in the MOF, the *trans* isomer adopts a planar, achiral form in solution, as verified experimentally. This shows that the chiral photoresolution is enabled by the linker reticulation in the MOF. Our study demonstrates the induction of chirality and optical activity in solid materials by CPL and opens new opportunities for chiral resolution and information storage with CPL.

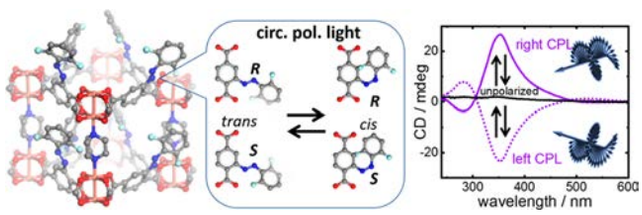

INTRODUCTION

Chirality is a central motif in nature and enantioselective molecular interactions are fundamental in biology, medicine, as well as agriculture.[1−4] Controlling chirality is crucial in many chemical processes, such as for directing the structure and functionality of various molecular assemblies.[5−8] In contrast to the use of chemical stimuli for chirality control,[5,8] the application of light as signal allows very fast remote switching with high spatial resolution. Thus, dynamic chirality control by molecules that undergo reversible isomerizations upon light irradiation is highly attractive. Different molecules with chiral and photoresponsive moieties have been shown to switch between different chiral isomers.[9,10] As examples, the chirality of metal complexes was controlled by unidirectional molecular rotary motors based on chiral overcrowded alkenes,[11] and chiral diarylethene compounds were used for photoswitchable chirality transfer.[12] In addition to switching the products in asymmetric catalysis, switching the chirality can also be used to switch the spin selectivity.[13] In these demonstrations, chiral moieties need to be installed within the photoswitchable molecules.

For starting with achiral materials and avoiding (initially) chiral moieties, a promising approach of inducing chirality and switching between different chiral isomers is based on the irradiation with circularly polarized light (CPL). CPL, as chiral electromagnetic radiation, can selectively interact with chiral molecules. This is used in circular dichroism (CD) spectroscopy for the enantiomer determination by enantioselective excitation and light absorption of right and left CPL. The selective excitation of chiral enantiomers by CPL has proven to be an effective means to induce enantioselective enrichment in asymmetric catalysis.[14−16] Enantioselective enrichment in prochiral photoswitchable compounds, such as azobenzene dimers and overcrowded alkenes, has also been realized by CPL.[17−21] For inducing chirality in materials, CPL has been used for rotating domains in polymers and liquid crystals.[22−25] The control of the chirality by CPL in solids, in particular in crystalline or nanoporous materials, has not yet been demonstrated.

The realization of solids with CPL induced chirality requires the incorporation of photoresponsive[26] molecules in the

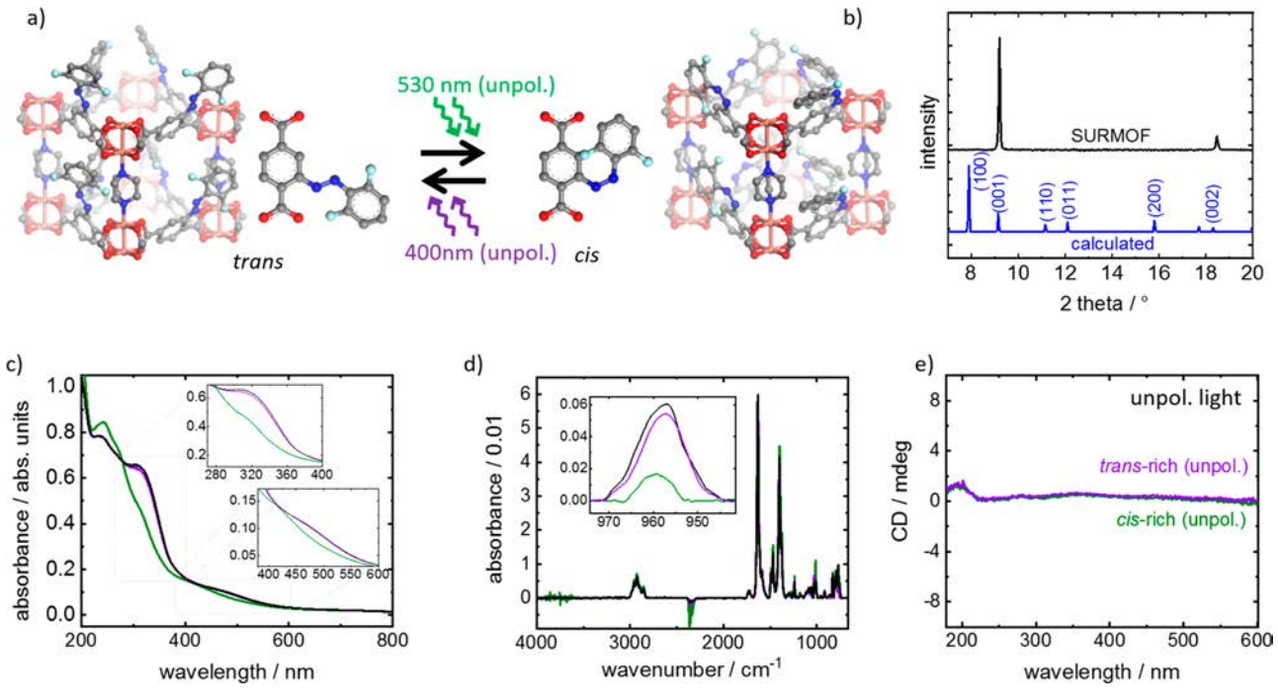

Figure 1. (a) Sketch of the $Cu_2(F_2AzoBDC)_2(dabco)$ SURMOF with the fluorinated azobenzene side groups that can be switched with light of 530 nm from *trans* (left) to *cis* (right) and back with 400 nm. One F_2AzoBDC linker molecule is shown next to the MOF unit cell. Carbon atoms are shown in gray, oxygen in red, copper in orange, fluorine in light blue, and nitrogen in blue. Hydrogen atoms have been omitted. (b) The XRD of the SURMOF compared with the calculated XRD of the targeted structure. The diffraction peaks are labeled. (c) UV−vis and (d) infrared reflection absorption spectra (IRRAS) of the SURMOF in the thermally relaxed state (black), where all azobenzene groups are in the *trans* state, upon irradiation with green light (green) and upon violet light irradiation (violet). For comparison, the UV−vis spectra of the linker in ethanolic solution are given in the Supporting Information (see Figure S1). (e) CD spectra of the SURMOF irradiated with unpolarized green and violet light, resulting in the *trans* rich (violet) and *cis* rich (green) states.

material without loss of molecular functionality. This can be realized by using metal−organic frameworks (MOFs).[27−29] MOFs are composed of organic ditopic or higher topic linker molecules connected by metal nodes. Using light responsive linker molecules can result in photoswitchable MOFs. The remote control of various MOF properties, including color, uptake, and diffusion as well as electronic and protonic conduction, was demonstrated for the material in the form of powder and thin films, illustrating that MOFs are indeed an attractive platform for photoswitchable materials.[30−35] Using the light responsive MOF material in the form of thin films has the advantage that the entire material is irradiated and the properties can be investigated by chiroptical methods in transmission mode.[36,37] For MOFs and other coordination networks, chirality transfer by means of chiral guest molecules in the pores or by chiral solvents during the synthesis was used to induce chirality in initially achiral frameworks.[7,38−41] Recently, it was demonstrated that the isomerization of achiral photoswitches induced by unpolarized light results in changes of the enantioselective adsorption properties in chiral MOFs.[42] There, the chirality of the material was not affected. Photoswitching of the chirality of the framework material itself has however not yet been demonstrated.

Here, we demonstrate the chirality induction in initially optically inactive crystalline nanoporous materials by using CPL. The material is based on MOFs with photoswitchable fluorinated azobenzene moieties, which can be reversibly switched by irradiation from their *trans* to their *cis* configuration with green light and *vice versa* using violet light. Upon irradiation with right or left CPL, this means clockwise or counterclockwise rotating CPL, bands in the CD spectra emerge, proving that the material becomes optically active. The induction of the optical activity is reversible and only depends on the handedness of the light. By detailed calculations, the molecular structure was unveiled and the observed CD bands can be assigned to the *R* and *S* forms of the *cis* and *trans* azobenzene isomers. While each individual molecule in the *cis* form is obviously chiral, we found that the *trans* azobenzene isomers in the MOF also adopt a nonplanar chiral form. To the best of our knowledge, this is the first demonstration of chirality induction and switching by CPL in solid materials.

EXPERIMENTAL SECTION

SURMOF synthesis: the thin MOF films were prepared in a layer by layer (lbl) fashion, resulting in surface mounted metal−organic frameworks (SURMOFs).[43,44] In detail, the pillared layer $Cu_2(F_2AzoBDC)_2(dabco)$ SURMOFs were synthesized by alter natively immersing a quartz glass substrate in the ethanolic solutions of the metal nodes (1 mM copper(II) acetate, Alfa Aesar) and of the organic linkers (0.2 mM 2 ((2,6 difluorophenyl)diazenyl) tereph thalic acid, referred to as F_2AzoBDC with the synthesis described in ref 45 and 1,4 diazabicyclo[2.2.2]octane, dabco, from Merck KGaA). The SURMOFs were prepared in 20 synthesis cycles. Prior to synthesis, the quartz glass substrate surface was cleaned by UV/ozone for 25 min. For the IR experiments, the samples are grown on gold substrates functionalized with a 11 mercapto 1 undecanol self assembled monolayer (MUD SAM). The lbl syntheses were performed by a dipping robot.[46] More details on the SURMOF synthesis can be found in ref 43.

The $Cu_2(F_2AzoBDC)_2(dabco)$ powder MOF was prepared following a standard solvothermal method.[47] A mixture of copper

nitrate ($Cu(NO_3)_2 \cdot 3H_2O$, 347.9 mg, 1.44 mmol), F_2AzoBDC (441.4 mg, 1.44 mmol), and dabco (80.8 mg, 0.72 mmol) was dissolved in DMF/ethanol (1:1 in volume, 200 mL) and kept at 100 °C for 48 h. The obtained MOF crystals were washed twice with DMF and *n* hexane and dried in dry nitrogen and stored under inert conditions.

X ray diffraction (XRD) measurements in out of plane geometry were carried out using a Bruker D8 Advance diffractometer with Cu anode and a wavelength of λ = 0.154 nm.

Scanning electron microscopy (SEM) and energy dispersive X ray spectroscopy (EDX) images were recorded with a TESCAN VEGA3 thermionic emission SEM system. The parameters are shown in the images in Figures S2 and S3.

Infrared spectra were recorded using a Bruker Vertex 80 Fourier Transform Infrared Reflection Absorption Spectrometer (FT IRRAS). The spectra were recorded in grazing incidence reflection mode at an angle of incidence of 80° relative to the surface normal.

UV−vis transmission spectra were recorded with a Cary5000 spectrometer from Agilent.

Solid state circular dichroism (CD) spectra of the SURMOF samples (i.e., Figures 1e, 2, 3, 6, and S7) were measured with a Jasco J 810 spectropolarimeter at room temperature. Spectra recorded for pure quartz glass plates (which were also used as the substrates for SURMOF thin film preparation) were used as reference background. Spectral scans were run from 600 to 180 nm in 0.5 nm steps using a 20 nm min^{-1} scan speed, a 4 s response time, and a spectral bandwidth of 1 nm. The circular quartz glass plate with the deposited

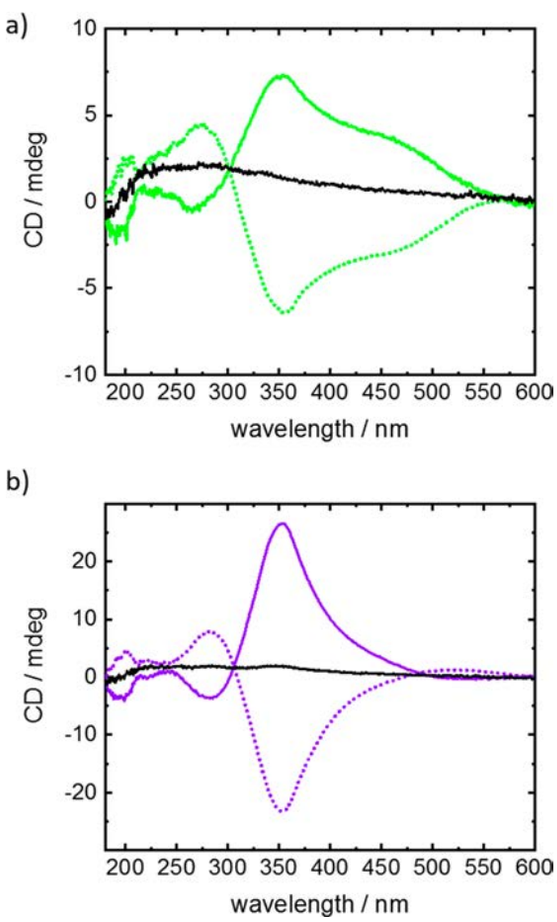

Figure 2. CD spectra of the $Cu_2(F_2AzoBDC)_2(dabco)$ SURMOF irradiated with right and left CPL of 530 nm (a) and 400 nm (b) wavelength. The spectra upon right CPL are shown as solid lines, the left CPL as dotted lines. The black lines in both plots are the spectra of the sample upon irradiation with unpolarized light of 530 nm (a) and 400 nm (b).

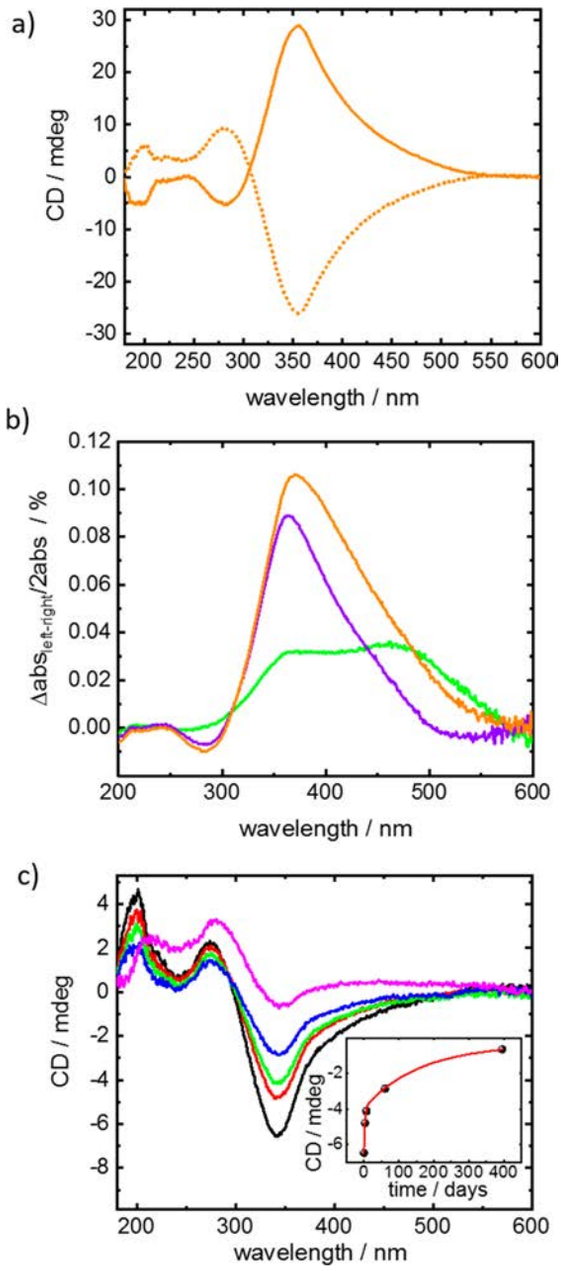

Figure 3. (a) CD spectra of the $Cu_2(F_2AzoBDC)_2(dabco)$ SURMOF irradiated with right and left CPL of both wavelengths simultaneously, i.e., 530 and 400 nm CPL combined (8 mW cm^{-2} at 400 nm and 5 mW cm^{-2} at 530 nm). The spectrum upon right CPL is shown as a solid line, and the left CPL spectrum is shown as a dotted line. (b) Spectra of the absorbance differences of left and right CPL, as measured by CD spectroscopy, divided by twice the total absorbance for the sample upon irradiation with right CPL of 400 nm (violet), 530 nm (green), and combined (orange). The maximum, corresponding to the enantiomeric excess in the photostationary state (ee_{PSS}), is 0.106% for orange, 0.089% for violet, and 0.035% for green. See Figure S8 for the corresponding UV−vis spectra. (c) CD spectra of the SURMOF during thermal relaxation at room temperature in the dark. Immediately upon mixed (green and violet light) left CPL (black), after 3 days (red), 7 days (green), 2 months (blue), and 13 months (violet). The inset shows the maximum at 340 nm versus time.

SURMOF sample was fixed perpendicular to the incident light beam on a rotation stage with a computer controlled stepping motor.[48] To

reduce artifacts due to linear dichroism or birefringence arising from imperfections in the sample or in the substrate (e.g., by slight vertical misalignment of the substrates or by strain in the quartz glass substrate), spectra were recorded every 45.0° of rotation of the sample around the light beam axis (i.e., 0°, 45°, 90°, 135°, 180°, 225°, 270°, and 315°) and averaged.[49] Absorption flattening artifacts were avoided by depositing only 20 layers of the SURMOF on the quartz glass substrate leading to absorbance values < 1, and potential light scattering issues were minimized by placing the sample at a distance of ~1 cm, i.e., as close as possible to the photomultiplier tube (PMT) detector of the J 810 spectropolarimeter to collect all forward scattered light.

Solid state CD measurements of $Cu_2(F_2AzoBDC)_2(dabco)$ MOF powder deposited by spin coating of a MOF suspension on the substrate, or of SURMOF reference samples without photoswitches, were performed in the same way.

The linear dichroism (LD) measurements of the SURMOF sample were also performed with the Jasco J 810 spectropolarimeter. There, the sample was not rotated. Linearly polarized light for the sample irradiation was produced by using a linear polarizer from Thorlabs. The sample was irradiated with light of 400 and 530 nm for 20 min each.

Solution CD (or liquid state CD) measurements of the SURMOF dissolved in organic solvent or of the pure F_2AzoBDC linker in ethanol solution (Figures 6 and S1b) were performed using a 1 mm quartz glass cuvette (SUPRASIL, Hellma Müllheim) using the same data acquisition parameters as described above.

The light irradiation of the sample was performed with LEDs from PrizMatix with wavelengths of 400 and 530 nm and maximum light power of 24 mW and 52 mW, respectively, corresponding to intensities of 8 and 17 mW cm^{-2}, respectively. The light intensity can be attenuated by a potentiometer at the LED box. For circularly polarized light (CPL) irradiation, right and left circular polarizers from Thorlabs were used. For all photoswitching processes, the samples were irradiated for 90 min, which is much longer than the time required for realizing the equilibrium state under similar conditions in previous studies, typically 5 to 10 min.[35,50] This means it is sufficiently long enough for reaching the photostationary state. All CD and UV−vis spectra (Figures 1c,e, 2, and 3) were obtained with one sample and subsequent irradiations. These spectra were reproduced with many other samples. All experiments were performed at room temperature.

Computational methods: all structural optimizations were performed using the Amsterdam Modeling Suite (AMS 2019).[51,52] The stereoisomers of the F_2AzoBDC molecule (Figure 4a−c) were optimized at the DFT level, using the dispersion corrected B3LYP D3(BJ) hybrid functional, Slater type all electron basis sets of TZP quality, and the implicit solvation model COSMO with ethanol as a solvent. Two MOF model structures, denoted *R,S trans* MOF and *R,S cis* MOF, were optimized in periodic boundary conditions (pbc) at the DFTB level using the GFN1 xTB method. The atomic positions were allowed to relax, while keeping the lattice parameters fixed at the experimental values. Finite cluster models were then cut from the optimized MOFs, such that each cluster model contains four copper paddlewheels linked via four F_2AzoBDC linkers, two of those representing the *R* (*trans* or *cis*) enantiomer and the other two, the *S* (*trans* or *cis*) enantiomer (Figure 4d,e). UV−vis and CD spectra of the F_2AzoBDC stereoisomers and the MOF cluster models were calculated using the sTD DFT method as implemented in Orca 4.2.1.[53] In the preceding ground state calculations, we used the dispersion corrected RS hybrid functional CAM B3LYP D3(BJ), with def2 SVP basis sets and def2/J auxiliary basis set, and the RIJCOSX approximation for the Coulomb and the HF Exchange integrals. More computational details are described in the Supporting Information.

RESULTS AND DISCUSSION

The $Cu_2(F_2AzoBDC)_2(dabco)$ SURMOF thin films with a pillared layer structure were prepared on quartz glass substrates in a layer by layer fashion. The X ray diffraction

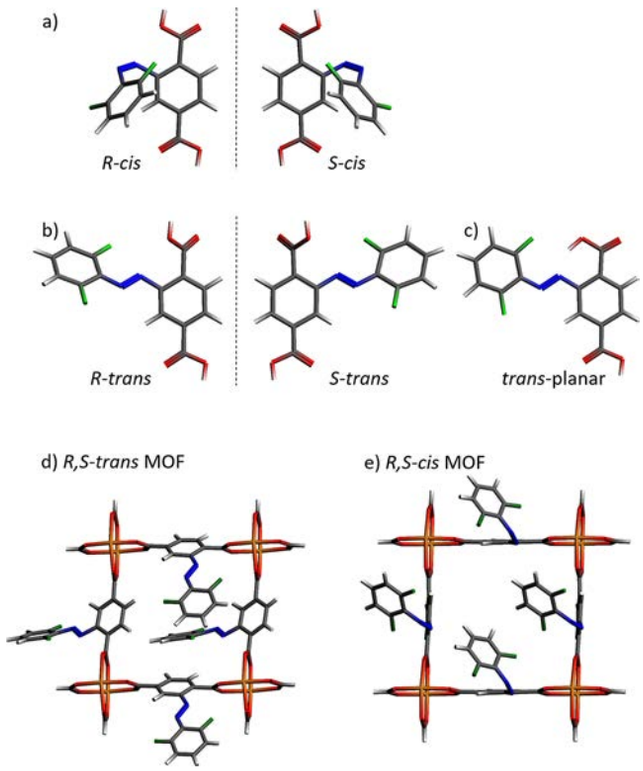

Figure 4. Stick representations of the molecular (a−c) and periodic (d,e) structure models of *cis* and *trans* stereoisomers of F_2AzoBDC. The *R* and *S* enantiomers of the *cis* form (a), the nonplanar *R* and *S* *trans* conformations (b) and the *trans* planar conformation (c) were optimized as free molecules at the B3LYP D3(BJ)/TZP/COSMO EtOH level of theory, using ADF 2019.[51] The dashed lines in (a) and (b) represent the mirror planes. The *R,S trans* MOF (d) and the *R,S cis* MOF (e) cluster models were cut from pbc optimized *R,S trans* MOF and *R,S cis* MOF, respectively, each containing equal amounts of the respective *R* and *S* conformers. The MOF structures were optimized using the GFN1 xTB method within the AMS 2019 driver,[51] while keeping the lattice parameters fixed at the experimental values. Color code: Cu, orange; F, green; O, red; N, blue; C, gray; H, white.

(XRD) data, Figure 1, show the films are crystalline having the targeted structures. In addition, the data show that the SURMOF films are grown in the [001] direction perpendicular to the substrate surface. Scanning electron microscopy (SEM) as well as photo and optical (microscopy) images are shown in Figure S2. The optical images show that the sample has a homogeneous (macroscopic) morphology. The SEM images show that the film is composed of many different intergrown crystallites and crystalline domains. The SEM images also show that the MOF film homogeneously covers the substrate with only a few pinholes. The film's thickness is approximately 0.2 μm. Elemental mapping via energy dispersive X ray spectroscopy (EDX) shows the homogeneous distribution of the significant elements, i.e., Cu, N, F and C, see Figure S3. The vibrational spectrum of the sample (Figure S4) also verifies the composition of the SURMOF film.

First, the photoisomerization with unpolarized light from a green (530 nm) and a violet (400 nm) LED was investigated. The UV−vis spectra of the SURMOF sample measured in the transmission mode show that the $\pi\pi^*$ band at 330 nm decreases upon green light irradiation and increases again upon subsequent violet light irradiation. In addition, the n π^* band

at approximately 450 nm shifts to shorter wavelengths upon irradiation with green light and to longer wavelengths after irradiation with violet light. Both findings are clear indication for green light induced *trans* to *cis* photoisomerization and violet light induced *cis* to *trans*, in agreement with previous work.[35,50] This is also in agreement with spectroscopic investigations of similar F_2 azobenzene molecules in solution showing wavelengths for the $\pi\,\pi^*$ excitation of the *trans* isomer at 309 nm and about 280 nm for the *cis* isomer as well as for the n π^* transition of the *trans* isomer at 451 nm and at 419 nm for the *cis* isomer.[54]

The CD spectra of the SURMOF upon irradiation with unpolarized green or violet light reveal no bands (Figure 1e). This shows that the SURMOF films are optically inactive and possess no (overall) chirality. The absence of chirality was expected since the MOF is composed entirely of achiral components.

The photostationary state (PSS) was further quantified by infrared reflection absorption spectroscopy, IRRAS. Initially, the sample is in the thermally relaxed state, that is 100% *trans*. The IRRA spectra (Figure 1d) show that upon green light irradiation a PSS is reached where 15% of the azobenzene moieties are in the *trans* state, this means 85% *cis*. This state is referred to as a *cis* rich state. Upon violet light irradiation, a PSS of 87% *trans* and 13% *cis* is reached, referred to as a *trans* rich state. We like to stress that the PSS is a result of permanent light induced *trans* to *cis* and *cis* to *trans* isomerization, where the PSS value at a given wavelength is given by the absorption cross sections σ and the quantum yields Φ, i.e., $PSS_{trans} = \sigma_{cis}\Phi_{cis\rightarrow trans}/(\sigma_{trans}\Phi_{trans\rightarrow cis} + \sigma_{cis}\Phi_{cis\rightarrow trans})$. This means under both green and violet light irradiation, both *trans* to *cis* and *cis* to *trans* photoisomerizations occur, however, with different probabilities. The situation becomes more complex for CPL irradiation of a chiral sample since the absorption cross sections of the *S* and *R* isomers differ from each other.

In the following, the SURMOF sample is irradiated with CPL. The CD spectra of the (initially optically inactive, *trans*) sample irradiated with right CPL and with left CPL of 530 nm wavelength, resulting in *cis* rich states, are shown in Figure 2a. The CD spectra show a clear Cotton effect, indicating optical activity of the material. In addition, the bands of the sample upon right CPL irradiation are opposite to the sample upon (subsequent) left CPL irradiation.

The CD spectra of the sample irradiated with right CPL and left CPL of 400 nm wavelength, resulting in *trans* rich states, are shown in Figure 2b. The bands of the right CPL and left CPL sample are again mirror images. In both sets of spectra, the strongest CD band is at about 350 nm. However, its intensity after violet CPL irradiation is significantly (about 4 times) larger than after green CPL irradiation.

As reference, the CD spectra of the F_2AzoBDC linker molecules dissolved in ethanol are measured upon CPL irradiation, Figure S1b. These spectra show that the pristine linker molecules in solution as well as upon CPL irradiations of 400 or 530 nm show no optical activity. Please note, these molecules clearly undergo photoisomerization, see Figure S1a.

As further reference, the CD spectra of a $Cu_2(BDC)_2$(dabco) SURMOF, i.e., a reference system without photoswichable azobenzene moieties, are shown in Figure S5. There, no optical activity upon CPL irradiation could be detected. This supports the hypothesis that the observed optical activity stems from the azobenzene groups.

The linear dichroism (LD) spectra of the $Cu_2(F_2AzoBDC)_2$(dabco) SURMOF upon irradiation with linearly polarized light of 530 and 400 nm, respectively, are shown in Figure S10. The intensities of the LD bands change reversibly upon irradiation with light of different wavelengths but identical polarizations. This is in clear contrast to photoalignment effects such as the Weigert effect in films of polymers or liquid crystals,[55,56] where the chromophores can reorient, inducing CD or LD, and back switching without changing the polarization is barely possible. This different behavior can be explained by structural differences. In contrast to photoalignment effects in polymers, the photoresponsive moieties in the SURMOF are firmly attached at the scaffold of the MOF, which is anchored on the substrate. As a result, the photoswitches in the SURMOF cannot freely rotate to a position with the transition dipole moment perpendicular to the plane of the exciting linearly polarized light.

The CD spectra of a $Cu_2(F_2AzoBDC)_2$(dabco) MOF powder, which was spin coated on a quartz glass substrate, were measured as further reference, Figure S6. There, upon CPL irradiation, CD bands similar to the CD bands measured for $Cu_2(F_2AzoBDC)_2$(dabco) SURMOF were observed. However, the signal intensity and the signal to noise ratio (and thus the signal quality) of the CD spectra of the MOF powder are significantly lower than of the MOF thin film (Figure S6b versus Figure 2), most likely due to the irregular morphology of the powder sample, see also the discussion in ref 57.

For the $Cu_2(F_2AzoBDC)_2$(dabco) SURMOF sample, in comparison to Figure 2, the intensity of the bands in the CD spectra can be further modulated by mixing the intensities of violet and green CPL (see Figure S7). The largest signal in the CD spectrum was recorded for the sample irradiated with a mixture of violet and green CPL (Figure 3a). The IRRA spectra (see Figure S9) reveal that approximately 75% of the azobenzene groups in this sample are in the *trans* state.

The enantiomeric excess in the photostationary state (ee_{PSS}) is given by $ee_{PSS} = \Delta\varepsilon/2\varepsilon$, where $\Delta\varepsilon$ is the difference of the molar extinction coefficients for left and right CPL and ε is the total molar extinction coefficient.[18,58] For a one species system (here the fluorinated azobenzene moieties in the MOF), the ratio $\Delta\varepsilon/2\varepsilon$ corresponds to the ratio of the absorbance $\Delta abs/2abs$, which follows from the CD and UV−vis absorption spectra. Please note, in case other components of the SURMOF sample also absorb in the respective spectrum range, $\sum$ the ratio $\Delta abs/2abs$ is smaller than $\Delta\varepsilon/2\varepsilon$ of the fluorinated azobenzene moieties. Thus, the ratio $\Delta abs/2abs$ serves as a lower limit for the ratio of the extinction coefficients ($\Delta\varepsilon/2\varepsilon$). In Figure 3b, the $\Delta abs/2abs$ values are plotted for the *trans* and *cis* rich state (shown in Figure 2) as well as for the optimized, mixed state (shown in Figure 3a). Here, an ee_{PSS} of up to 0.106% is realized. Such an enantiomeric excess is comparable to CPL induced photoresolution processes in solution.[18,58]

The optical activity of the sample remains for a long time. The CD spectra of a sample measured over a period of 13 months are shown in Figure 3c. The decrease of the intensity of the CD band at 350 nm can be best described with a two component exponential decay function with time constants of about 3 days and 160 days. This shows that the chiral isomers in the MOF are rather stable.

All CD spectra show an intense band at about 350 nm and tail out to longer wavelengths. Comparing the bands in the CD

spectra with the positions of the $\pi\,\pi^*$ and n π^* excitation of the azobenzene moieties shows that the CD spectra cannot be explained only by chiral *cis* azobenzene isomers. The wavelength of the strong CD band (350 nm) corresponds approximately to the wavelength of the *trans* $\pi\,\pi^*$ excitation. The shoulder at longer wavelengths may be a combination of the n π^* excitation bands of the *trans* and *cis* isomers, at approximately 420 and 450 nm. As a result, the CD data indicate that there exist stable chiral forms of both isomers, *trans* and *cis*.

To better understand the experimentally observed light induced phenomena in the $Cu_2(F_2AzoBDC)_2(dabco)$ SUR MOF, we performed first principles calculations employing molecular as well as periodic structure models representing both the *cis* and the *trans* configurations of the fluorinated azobenzene moieties. The density functional theory (DFT) (see Methods and the Supporting Information for details) calculations for the *cis* F_2AzoBDC linker molecule confirm its chiral nature by finding two isoenergetic local minima on the potential energy surface (PES). These local minimum structures are nonsuperimposable mirror images of each other and can be designated as right handed and left handed enantiomers (Figure 4a). The *R cis* and *S cis* enantiomers are predicted to be approximately 24 kJ mol^{-1} less stable than the two isoenergetic nonplanar *trans* conformers, denoted *R trans* and *S trans* (Figure 4b). An essentially planar *trans* conformer was found to be even more stable (by 30 kJ mol^{-1}) than the nonplanar *trans* conformers (Table S1). Its planar structure is stabilized by the formation of a hydrogen bond between one of the nitrogen atoms and the hydrogen from the *ortho* carboxyl group of the terephthalate moiety (Figure 4c). The *cis* and the nonplanar *trans* isomers display axial (or helical) chirality, and therefore, the respective enantiomers are labeled *R* and *S* (or *P* and *M*).

Our calculations show that once the *trans* F_2AzoBDC is incorporated as a linker in the MOF structure, the deviation from a planar conformation is greatly enhanced. Indeed, a planar conformation of the *trans* F_2AzoBDC linkers could not be stabilized due to the absence of carboxylic hydrogen atoms in the MOF structure. A stable nonplanar *trans* form in a similar azobenzene MOF structure was also theoretically predicted with the help of atomistic simulations by others recently.[59] Within the pore of a *trans* MOF having initially equal amount of *R trans* and *S trans* linker conformations, the fluorinated azobenzene moieties are oriented rather close to each other (Figure 4d), and due to the induced dispersion interactions between the closely lying aromatic groups, conformations with diverse deviation from planarity were stabilized (see Table S2). In other words, the spatial confinement of *trans* F_2AzoBDC as a building unit of the framework structure drastically reduces the probability for the presence of the (achiral) planar conformation. This greatly enhances the probability for the presence of various nonplanar (and intrinsically chiral) conformations with much more diverse deviation from planarity, as compared to the free *trans* F_2AzoBDC molecules in solution (see Table S2).

Contrary to *cis* F_2AzoBDC, neither of the three *trans* configured conformers could be verified as a true local PES minimum at the computational level used. All *trans* species have one extremely low imaginary frequency (see Table S1) corresponding, in the case of nonplanar *R* and *S trans*, to an in plane and, in the case of *trans* planar, to an out of plane motion of the two aromatic moieties in F_2AzoBDC with respect to the N═N bridge. This is a clear indication that *trans* F_2AzoBDC exhibits pronounced structural flexibility in terms of spatial orientation of the aromatic substituents with respect to the N═N bond, which in turn implies that its solution state might be a mixture of various *trans* conformers (see Table S2).

This hypothesis is further supported by the sTD DFT calculated UV−vis spectra of the F_2AzoBDC molecules (Figure 5a). For the *trans* conformation, an excellent

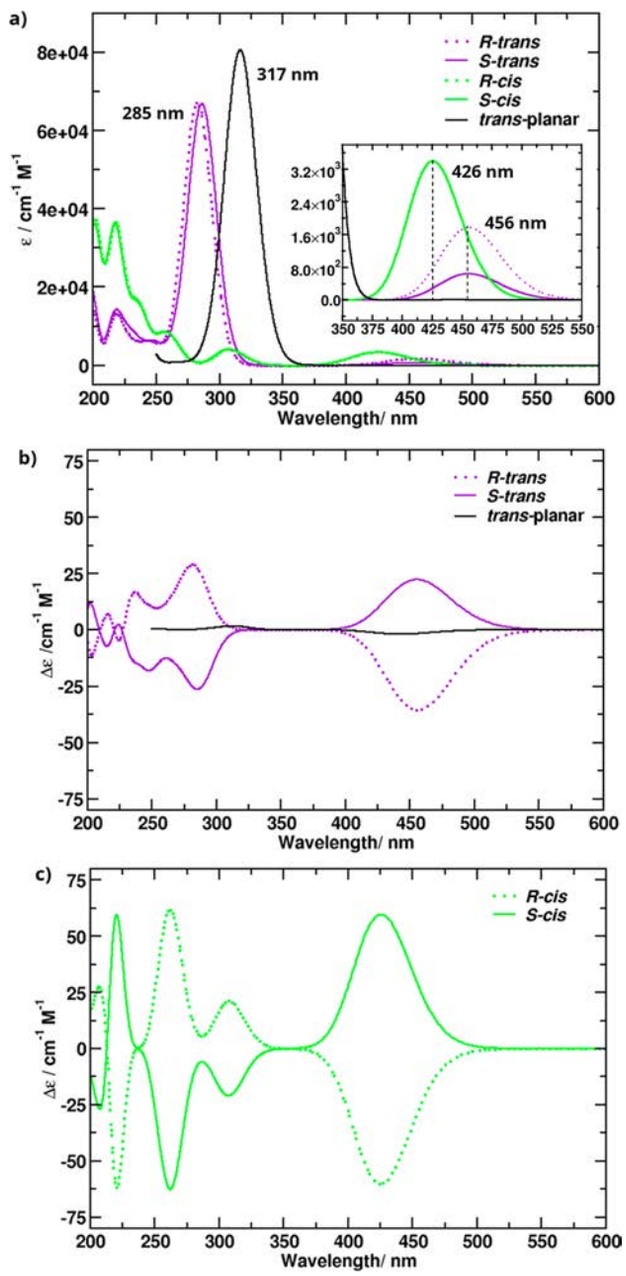

Figure 5. Calculated UV−vis spectra (a) and CD spectra (b,c) for the *R* and *S* enantiomers of *cis* (green lines), the nonplanar *R* and *S* conformers of *trans* (violet lines), and the planar *trans* conformer (black lines) of F_2AzoBDC. sTD DFT (CAM B3LYP D3(BJ)/def2 SVP) calculations in the gas phase with ORCA 4.2.1,[53] for the DFT optimized (B3LYP D3(BJ)/TZP/COSMO EtOH) molecular structures. Gaussian root mean square width of 0.15 eV is used for line broadening.

agreement with the experimentally measured peak positions (see Figures 1 and S1) is achieved only when taking into account the predictions for both the nonplanar (Figure 4b) and the planar (Figure 4c) conformers. The n π^* band, calculated for the nonplanar *R* and *S trans* at 456 nm (compared to 450 nm in the experiment), becomes slightly blue shifted but, most importantly, symmetry forbidden for *trans* planar. On the other hand, the $\pi-\pi^*$ band at 317 nm, as predicted for *trans* planar, agrees very well with the experimental value, whereas a blue shift of ca. 30 nm is predicted for the two nonplanar conformers (see Figure 5a and Table S3 for details about the calculated transitions and visualization of the major orbital contributions).

The sTD DFT calculated CD spectra of the nonplanar *R trans* and *S trans* F_2AzoBDC (Figure 5b) are rather similar, having peak intensities of opposite sign and slightly different magnitude. The subtle differences in the optical response of *R trans* and *S trans* could be well explained with the structural flexibility of the *trans* molecules, as evidenced by the slightly different torsion of the two aromatic substituents with respect to the bridging N═N bond in F_2AzoBDC amounting to 34° for *S trans* and 45° for *R trans* (see Table S2). As expected, the calculated CD spectrum for the achiral *trans* planar conformer is essentially zero.

On the other hand, the *R* and *S* enantiomers of the *cis* F_2AzoBDC isomer are perfect mirror images of each other and, consequently, have indistinguishable UV−vis spectra (Figure 5a). Compared to the *trans* species, the intensity of the $\pi-\pi^*$ band is decreased and the n π^* and π π^* bands are blue shifted, in agreement with the experimental findings (see Figures 1 and S1). As expected, the calculated CD spectra of *R cis* and *S cis* (Figure 5c) are of exactly the same shape and magnitude but with opposite sign. Interestingly, in the CD spectra, the predicted intensities of the *cis* enantiomers are about twice as large as of the nonplanar *trans* conformers.

On the grounds of the computational findings, we conclude that in the symmetric (achiral) environment, the (common) state of *cis* F_2AzoBDC constitutes a racemic mixture of 50% *R cis* and 50% *S cis*, which upon irradiation with unpolarized light (UPL) will show no optical activity. Furthermore, the CD spectrum predicted for a model structure of a *cis* MOF with equal amount of *R cis* and *S cis* F_2AzoBDC linkers, i.e., *cis* MOF racemate (Figure 4e), is essentially zero (Figure S11a). This is in agreement with the experimentally verified optically inactive behavior upon UPL irradiation (see Figure 1e). As for the *trans* F_2AzoBDC, its solution state most probably contains the hydrogen bonded planar conformer (see Figure 4c), as well as nonplanar conformers with various torsion of the aromatic groups with respect to the N═N bridge (e.g., Figure 4b), thus contributing altogether to an overall achiral behavior. The calculations clearly show that *trans* and *cis* F_2AzoBDC have stable chiral isomers. This supports the hypothesis that the optical activity of the MOF films, both in their *trans* and *cis* forms, can be switched on via CPL irradiation by triggering partial photoresolution, which causes deracemization and enrichment of one of the possible nonplanar *trans* conformers, or one of the two *cis* enantiomers of F_2AzoBDC.

By comparing the calculation results with the experimental CD spectra (see Figures 2 and 3), we conclude that the sample obtained after right CPL irradiation has an excess of *S trans* and *S cis* isomers. Vice versa, the sample upon the left CPL has *R* isomer enrichment. This means that the right CPL has a stronger interaction with the *R* isomers, causing a more frequent excitation and depletion of the *R* isomers. As a result, the *S* isomers are enriched and *vice versa* for left CPL. The strong intensity of the CD bands at 350 nm and only small CD bands (or shoulder) at 450 nm indicate that the majority of enantiomer enriched isomers is in the *trans* rather than the *cis* form.

Moreover, the calculations predict that the most stable *trans* form in solution is planar, while it is nonplanar in the MOF. To experimentally validate this computational finding, we prepared a SURMOF and induced chiral enrichment by CPL, clearly verified by the CD spectrum (Figure 6, black line). Subsequently, this sample was dissolved in an acidic aqueous ethanol solution. The CD spectrum of the dissolved MOF (Figure 6, red line) is essentially zero, indicating that the molecules possess no optical activity. This verifies the theoretical prediction that the most stable form of the F_2Azo BDC molecule in solution has a planar conformation and therefore is achiral. As the bottom line, the optical activity of the material is a result of the reticulation of the linker molecules in the MOF scaffold. This conclusion is also supported by the reference experiments with the linker molecules in solution (Figure S1), with the MOF powder of the same structure (Figure S6) and with a SURMOF film without photoswitchable azobenzene moieties (Figure S5).

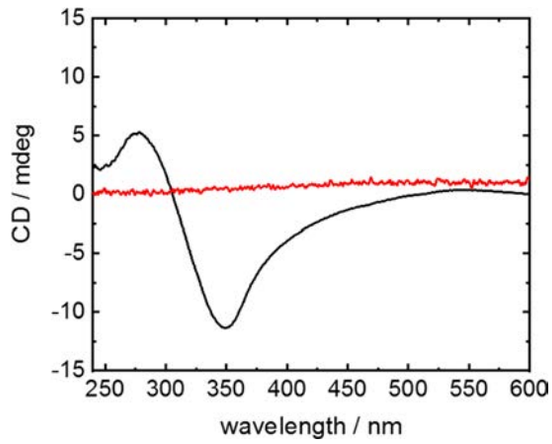

Figure 6. CD spectra of the SURMOF upon left CPL irradiation (black; simultaneously irradiated with green and violet light, see Figure 3a,b) and subsequently dissolved (red). The SURMOF, with an area of 3.1 cm^2, was dissolved in 1 mL of a solution of ethanol, water, and acetic acid (1:1:1) and measured in a cuvette of 1 mm thickness.

CONCLUSION

We demonstrate that circularly polarized light can induce stable optical activity in a solid crystalline material. The material is based on crystalline, nanoporous metal−organic frameworks with photoswitchable fluorinated azobenzene side groups pending at the scaffold. By using thin MOF films, the UV−vis and CD spectra can be measured in the transmission mode, allowing one to quantify the optical activity. Depending on the CPL handedness, *R* or *S* azobenzene isomers in the material are enriched, causing optical activity of the material. The switching is fully reversible. DFT calculations show that both, *trans* and *cis,* forms possess chiral isomers in the MOF. By right CPL irradiation, the *R* isomers are excited, resulting in an enrichment of the *S* isomers, and *vice versa* for left CPL.

The induction of the optical activity in the material is also a result of the reticulation of the photoswitchable linker in the MOF scaffold and cannot be observed for the free photo switches in solution.

We believe the dynamic switching of the chirality can also be applied to other photoswitchable nanoporous materials based on photochromic moieties such as spiropyrans[34,60] and diarylethenes.[61,62] Such materials may enable photoswitchable membranes[63] with remote controllable enantioselective per meation. The switching of the optical activity may also find application in information processing based on CPL.[64]

AUTHOR INFORMATION

Corresponding Author

Lars Heinke − *Institute of Functional Interfaces (IFG), Karlsruhe Institute of Technology (KIT), 76344 Eggenstein Leopoldshafen, Germany;* orcid.org/0000 0002 1439 9695; Email: Lars.Heinke@KIT.edu

Authors

Anemar Bruno Kanj − *Institute of Functional Interfaces (IFG), Karlsruhe Institute of Technology (KIT), 76344 Eggenstein Leopoldshafen, Germany;* orcid.org/0000 0001 6385 4634

Jochen Bürck − *Institute of Biological Interfaces (IBG 2), Karlsruhe Institute of Technology (KIT), 76344 Eggenstein Leopoldshafen, Germany;* orcid.org/0000 0002 2256 9498

Nina Vankova − *Fakultät für Chemie und Lebensmittelchemie, TU Dresden, 01062 Dresden, Germany*

Chun Li − *Institute of Functional Interfaces (IFG), Karlsruhe Institute of Technology (KIT), 76344 Eggenstein Leopoldshafen, Germany*

Dragos Mutruc − *Department of Chemistry & IRIS Adlershof, Humboldt Universität zu Berlin, 12489 Berlin, Germany*

Abhinav Chandresh − *Institute of Functional Interfaces (IFG), Karlsruhe Institute of Technology (KIT), 76344 Eggenstein Leopoldshafen, Germany*

Stefan Hecht − *Department of Chemistry & IRIS Adlershof, Humboldt Universität zu Berlin, 12489 Berlin, Germany; DWI Leibniz Institute for Interactive Materials, 52074 Aachen, Germany; Institute of Technical and Macromolecular Chemistry, RWTH Aachen University, 52074 Aachen, Germany;* orcid.org/0000 0002 6124 0222

Thomas Heine − *Fakultät für Chemie und Lebensmittelchemie, TU Dresden, 01062 Dresden, Germany; Forschungsstelle Leipzig, Helmholtz Zentrum Dresden Rossendorf, 04318 Leipzig, Germany;* orcid.org/0000 0003 2379 6251

Notes

The authors declare no competing financial interest.

[Σ]The intensity of typical absorption bands of such MOF materials, like ligand to metal charge transfer absorption of the Cu nodes in the UV range and its tail out to the visible range (see ref 65) seem to be small in the respective range of the visible spectra of the sample, see Figure 1c.

ACKNOWLEDGMENTS

The authors gratefully acknowledge funding by the Volkswa gen Foundation and the German Science Foundation (DFG via BL 1269 "Visimat", HE 7036/5, and SPP 1928 "COORNETs"). We thank the Center for Information Services and High Performance Computing (ZIH) at TU Dresden for computational resources. We thank Bianca Posselt (KIT) for technical assistance in the CD and LD measure ments.

REFERENCES

(1) Green, D. W.; Lee, J. M.; Kim, E. J.; Lee, D. J.; Jung, H. S. Chiral Biomaterials: From Molecular Design to Regenerative Medicine. *Adv. Mater. Interfaces* **2016**, *3* (6), 1500411.

(2) Yashima, E.; Maeda, K.; Iida, H.; Furusho, Y.; Nagai, K. Helical Polymers: Synthesis, Structures, and Functions. *Chem. Rev.* **2009**, *109* (11), 6102−6211.

(3) Barron, L. D. Chirality and life. *Space Sci. Rev.* **2008**, *135* (1−4), 187−201.

(4) Agranat, I.; Caner, H.; Caldwell, A. Putting chirality to work: The strategy of chiral switches. *Nat. Rev. Drug Discovery* **2002**, *1* (10), 753−768.

(5) Miyake, H.; Tsukube, H. Coordination chemistry strategies for dynamic helicates: time programmable chirality switching with labile and inert metal helicates. *Chem. Soc. Rev.* **2012**, *41* (21), 6977−6991.

(6) Pijper, D.; Feringa, B. L. Control of dynamic helicity at the macro and supramolecular level. *Soft Matter* **2008**, *4* (7), 1349−1372.

(7) Crassous, J. Chiral transfer in coordination complexes: towards molecular materials. *Chem. Soc. Rev.* **2009**, *38* (3), 830−845.

(8) Meudtner, R. M.; Hecht, S. Helicity inversion in responsive foldamers induced by achiral halide ion guests. *Angew. Chem., Int. Ed.* **2008**, *47* (26), 4926−4930.

(9) Petermayer, C.; Dube, H. Circular Dichroism Photoswitching with a Twist: Axially Chiral Hemiindigo. *J. Am. Chem. Soc.* **2018**, *140* (42), 13558−13561.

(10) Feringa, B. L.; van Delden, R. A.; Koumura, N.; Geertsema, E. M. Chiroptical Molecular Switches. *Chem. Rev.* **2000**, *100* (5), 1789−1816.

(11) Zhao, D.; van Leeuwen, T.; Cheng, J.; Feringa, B. L. Dynamic control of chirality and self assembly of double stranded helicates with light. *Nat. Chem.* **2017**, *9*, 250.

(12) Jurissek, C.; Berger, F.; Eisenreich, F.; Kathan, M.; Hecht, S. External Reversal of Chirality Transfer in Photoswitches. *Angew. Chem., Int. Ed.* **2019**, *58* (7), 1945−1949.

(13) Suda, M.; Thathong, Y.; Promarak, V.; Kojima, H.; Nakamura, M.; Shiraogawa, T.; Ehara, M.; Yamamoto, H. M. Light driven molecular switch for reconfigurable spin filters. *Nat. Commun.* **2019**, *10*, 7.

(14) Sato, I.; Sugie, R.; Matsueda, Y.; Furumura, Y.; Soai, K. Asymmetric synthesis utilizing circularly polarized light mediated by the photoequilibrium of chiral olefins in conjunction with asymmetric autocatalysis. *Angew. Chem., Int. Ed.* **2004**, *43* (34), 4490−4492.

(15) Richardson, R. D.; Baud, M. G. J.; Weston, C. E.; Rzepa, H. S.; Kuimova, M. K.; Fuchter, M. J. Dual wavelength asymmetric photochemical synthesis with circularly polarized light. *Chem. Sci.* **2015**, *6* (7), 3853−3862.

(16) Kuhn, W.; Knopf, E. Photochemische Erzeugung optisch aktiver Stoffe. *Naturwissenschaften* **1930**, *18* (8), 183−183.

(17) Rijeesh, K.; Hashim, P. K.; Noro, S.; Tamaoki, N. Dynamic induction of enantiomeric excess from a prochiral azobenzene dimer under circularly polarized light. *Chem. Sci.* **2015**, *6* (2), 973−980.
(18) Hashim, P. K.; Tamaoki, N. Enantioselective Photochromism under Circularly Polarized Light. *ChemPhotoChem.* **2019**, *3* (6), 347−355.
(19) Bisoyi, H. K.; Li, Q. Light Directing Chiral Liquid Crystal Nanostructures: From 1D to 3D. *Acc. Chem. Res.* **2014**, *47* (10), 3184−3195.
(20) Hashim, P. K.; Thomas, R.; Tamaoki, N. Induction of Molecular Chirality by Circularly Polarized Light in Cyclic Azobenzene with a Photoswitchable Benzene Rotor. *Chem. Eur. J.* **2011**, *17* (26), 7304−7312.
(21) Huck, N. P. M.; Jager, W. F.; deLange, B.; Feringa, B. L. Dynamic control and amplification of molecular chirality by circular polarized light. *Science* **1996**, *273* (5282), 1686−1688.
(22) Burnham, K. S.; Schuster, G. B. Transfer of chirality from circularly polarized light to a bulk material property: Propagation of photoresolution by a liquid crystal transition. *J. Am. Chem. Soc.* **1999**, *121* (43), 10245−10246.
(23) Iftime, G.; Labarthet, F. L.; Natansohn, A.; Rochon, P. Control of chirality of an azobenzene liquid crystalline polymer with circularly polarized light. *J. Am. Chem. Soc.* **2000**, *122* (51), 12646−12650.
(24) Li, J.; Schuster, G. B.; Cheon, K. S.; Green, M. M.; Selinger, J. V. Switching a helical polymer between mirror images using circularly polarized light. *J. Am. Chem. Soc.* **2000**, *122* (11), 2603−2612.
(25) Hore, D. K.; Natansohn, A. L.; Rochon, P. L. The characterization of photoinduced chirality in a liquid crystalline azo polymer on irradiation with circularly polarized light. *J. Phys. Chem. B* **2003**, *107* (11), 2506−2518.
(26) Feringa, B. L.; Browne, W. R. *Molecular Switches*; Wiley, 2011; p 792.
(27) Furukawa, H.; Cordova, K. E.; O'Keeffe, M.; Yaghi, O. M. The Chemistry and Applications of Metal Organic Frameworks. *Science* **2013**, *341* (6149), 1230444.
(28) Ferey, G. Hybrid porous solids: past, present, future. *Chem. Soc. Rev.* **2008**, *37* (1), 191−214.
(29) Kaskel, S. *The Chemistry of Metal Organic Frameworks: Synthesis, Characterization, and Applications*; Wiley, 2016; p 904.
(30) Modrow, A.; Zargarani, D.; Herges, R.; Stock, N. Introducing a photo switchable azo functionality inside Cr MIL 101 NH_2 by covalent post synthetic modification. *Dalt. Trans.* **2012**, *41* (28), 8690−8696.
(31) Bigdeli, F.; Lollar, C. T.; Morsali, A.; Zhou, H. C. Switching in Metal Organic Frameworks. *Angew. Chem., Int. Ed.* **2020**, *59* (12), 4652−4669.
(32) Yanai, N.; Uemura, T.; Inoue, M.; Matsuda, R.; Fukushima, T.; Tsujimoto, M.; Isoda, S.; Kitagawa, S. Guest to Host Transmission of Structural Changes for Stimuli Responsive Adsorption Property. *J. Am. Chem. Soc.* **2012**, *134* (10), 4501−4504.
(33) Mutruc, D.; Goulet Hanssens, A.; Fairman, S.; Wahl, S.; Zimathies, A.; Knie, C.; Hecht, S. Modulating Guest Uptake in Core Shell MOFs with Visible Light. *Angew. Chem., Int. Ed.* **2019**, *58*, 12862−12867.
(34) Kanj, A. B.; Chandresh, A.; Gerwien, A.; Grosjean, S.; Bräse, S.; Wang, Y.; Dube, H.; Heinke, L. Proton conduction photomodulation in spiropyran functionalized MOFs with large on off ratio. *Chem. Sci.* **2020**, *11* (5), 1404−1410.
(35) Müller, K.; Helfferich, J.; Zhao, F. L.; Verma, R.; Kanj, A. B.; Meded, V.; Bléger, D.; Wenzel, W.; Heinke, L. Switching the Proton Conduction in Nanoporous, Crystalline Materials by Light. *Adv. Mater.* **2018**, *30* (8), 1706551.
(36) Haldar, R.; Heinke, L.; Wöll, C. Advanced Photoresponsive Materials Using the Metal Organic Framework Approach. *Adv. Mater.* **2020**, *32*, 1905227.
(37) Li, C.; Heinke, L. Thin Films of Homochiral Metal Organic Frameworks for Chiroptical Spectroscopy and Enantiomer Separation. *Symmetry* **2020**, *12* (5), 686.
(38) Das, S.; Xu, S. X.; Ben, T.; Qiu, S. L. Chiral Recognition and Separation by Chirality Enriched Metal Organic Frameworks. *Angew. Chem., Int. Ed.* **2018**, *57* (28), 8629−8633.
(39) Xia, Z.; Jing, X.; He, C.; Wang, X.; Duan, C. Coordinative Alignment of Chiral Molecules to Control over the Chirality Transfer in Spontaneous Resolution and Asymmetric Catalysis. *Sci. Rep.* **2017**, *7* (1), 15418.
(40) Verma, A.; Tomar, K.; Bharadwaj, P. K. Chiral Cadmium(II) Metal Organic Framework from an Achiral Ligand by Spontaneous Resolution: An Efficient Heterogeneous Catalyst for the Strecker Reaction of Ketones. *Inorg. Chem.* **2017**, *56* (22), 13629−13633.
(41) Berijani, K.; Morsali, A.; Hupp, J. T. An effective strategy for creating asymmetric MOFs for chirality induction: a chiral Zr based MOF for enantioselective epoxidation. *Catal. Sci. Technol.* **2019**, *9* (13), 3388−3397.
(42) Kanj, A. B.; Buerck, J.; Grosjean, S.; Braese, S.; Heinke, L. Switching the enantioselectivity of nanoporous host materials by light. *Chem. Commun.* **2019**, *55* (60), 8776−8779.
(43) Shekhah, O.; Wang, H.; Kowarik, S.; Schreiber, F.; Paulus, M.; Tolan, M.; Sternemann, C.; Evers, F.; Zacher, D.; Fischer, R. A.; Wöll, C. Step by step route for the synthesis of metal organic frameworks. *J. Am. Chem. Soc.* **2007**, *129* (49), 15118−15119.
(44) Heinke, L.; Wöll, C. Surface Mounted Metal Organic Frame works: Crystalline and Porous Molecular Assemblies for Fundamental Insights and Advanced Applications. *Adv. Mater.* **2019**, *31* (26), 1806324.
(45) Castellanos, S.; Goulet Hanssens, A.; Zhao, F.; Dikhtiarenko, A.; Pustovarenko, A.; Hecht, S.; Gascon, J.; Kapteijn, F.; Bleger, D. Structural Effects in Visible Light Responsive Metal Organic Frame works Incorporating ortho Fluoroazobenzenes. *Chem. Eur. J.* **2016**, *22* (2), 746−752.
(46) Gu, Z. G.; Pfriem, A.; Hamsch, S.; Breitwieser, H.; Wohlgemuth, J.; Heinke, L.; Gliemann, H.; Woll, C. Transparent films of metal organic frameworks for optical applications. *Micro porous Mesoporous Mater.* **2015**, *211*, 82−87.
(47) Wannapaiboon, S.; Schneemann, A.; Hante, I.; Tu, M.; Epp, K.; Semrau, A. L.; Sternemann, C.; Paulus, M.; Baxter, S. J.; Kieslich, G.; Fischer, R. A., Control of structural flexibility of layered pillared metal organic frameworks anchored at surfaces. *Nat. Commun.* **2019**, *10*, DOI: 10.1038/s41467 018 08285 5.
(48) Gu, Z. G.; Bürck, J.; Bihlmeier, A.; Liu, J.; Shekhah, O.; Weidler, P. G.; Azucena, C.; Wang, Z.; Heissler, S.; Gliemann, H.; Klopper, W.; Ulrich, A. S.; Wöll, C. Oriented Circular Dichroism Analysis of Chiral Surface Anchored Metal Organic Frameworks Grown by Liquid Phase Epitaxy and upon Loading with Chiral Guest Compounds. *Chem. Eur. J.* **2014**, *20* (32), 9879−9882.
(49) Castiglioni, E.; Biscarini, P.; Abbate, S. Experimental Aspects of Solid State Circular Dichroism. *Chirality* **2009**, *21* (1E), E28−E36.
(50) Müller, K.; Knebel, A.; Zhao, F.; Bléger, D.; Caro, J.; Heinke, L. Switching Thin Films of Azobenzene Containing Metal Organic Frameworks with Visible Light. *Chem. Eur. J.* **2017**, *23*, 5434−5438.
(51) te Velde, G.; Bickelhaupt, F. M.; Baerends, E. J.; Fonseca Guerra, C.; van Gisbergen, S. J. A.; Snijders, J. G.; Ziegler, T. Chemistry with ADF. *J. Comput. Chem.* **2001**, *22* (9), 931−967.
(52) ADF 2019: SCM *Software for Chemistry & Materials; Theoretical Chemistry*; Vrije Universiteit: Amsterdam, The Nether lands, 2019, http://www.scm.com (accessed 14 Apr, 2021).
(53) Neese, F. The ORCA program system. *Wiley Interdiscip. Rev.: Comput. Mol. Sci.* **2012**, *2* (1), 73−78.
(54) Knie, C.; Utecht, M.; Zhao, F. L.; Kulla, H.; Kovalenko, S.; Brouwer, A. M.; Saalfrank, P.; Hecht, S.; Bleger, D. ortho Fluoroazobenzenes: Visible Light Switches with Very Long Lived Z Isomers. *Chem. Eur. J.* **2014**, *20* (50), 16492−16501.
(55) Choi, S. W.; Kawauchi, S.; Ha, N. Y.; Takezoe, H. Photoinduced chirality in azobenzene containing polymer systems. *Phys. Chem. Chem. Phys.* **2007**, *9* (28), 3671−3681.
(56) Ikeda, T. Photomodulation of liquid crystal orientations for photonic applications. *J. Mater. Chem.* **2003**, *13* (9), 2037−2057.

(57) Haldar, R.; Heinke, L.; Woll, C. Advanced Photoresponsive Materials Using the Metal Organic Framework Approach. *Adv. Mater.* **2020**, *32* (20), 1905227.
(58) Feringa, B. L.; van Delden, R. A. Absolute asymmetric synthesis: The origin, control, and amplification of chirality. *Angew. Chem., Int. Ed.* **1999**, *38* (23), 3418.
(59) Kolodzeiski, E.; Amirjalayer, S. Atomistic Insight Into the Host Guest Interaction of a Photoresponsive Metal Organic Framework. *Chem. Eur. J.* **2020**, *26* (6), 1263−1268.
(60) Kortekaas, L.; Browne, W. R. The evolution of spiropyran: fundamentals and progress of an extraordinarily versatile photo chrome. *Chem. Soc. Rev.* **2019**, *48* (12), 3406−3424.
(61) Irie, M.; Fukaminato, T.; Matsuda, K.; Kobatake, S. Photochromism of Diarylethene Molecules and Crystals: Memories, Switches, and Actuators. *Chem. Rev.* **2014**, *114* (24), 12174−12277.
(62) Patel, D. G.; Walton, I. M.; Cox, J. M.; Gleason, C. J.; Butzer, D. R.; Benedict, J. B. Photoresponsive porous materials: the design and synthesis of photochromic diarylethene based linkers and a metal organic framework. *Chem. Commun.* **2014**, *50* (20), 2653−2656.
(63) Wang, Z.; Knebel, A.; Grosjean, S.; Wagner, D.; Bräse, S.; Wöll, C.; Caro, J.; Heinke, L. Tunable molecular separation by nanoporous membranes. *Nat. Commun.* **2016**, *7*, 13872.
(64) Yang, Y.; da Costa, R. C.; Fuchter, M. J.; Campbell, A. J. Circularly polarized light detection by a chiral organic semiconductor transistor. *Nat. Photonics* **2013**, *7* (8), 634−638.
(65) Gu, Z.; Heinke, L.; Wöll, C.; Neumann, T.; Wenzel, W.; Li, Q.; Fink, K.; Gordan, O. D.; Zahn, D. R. T. Experimental and theoretical investigations of the electronic band structure of metal organic frameworks of HKUST 1 type. *Appl. Phys. Lett.* **2015**, *107*, 183301.